

Modern electric vehicles typically exploit synchronous motors with magnetoelectric excitation as traction engines. While possessing a series of undeniable advantages, the synchronous motor has one significant drawback – the high cost predetermined by the high price of permanent magnets. In addition, the impossibility to disable a magnetic field in case of engine malfunction can lead to an emergency on the road. Given this, there is a need to design new structures of electrical machines with electromagnetic excitation.

The structure of a DC traction motor with electromagnetic excitation involving the rotor or stator segmentation makes it possible to considerably weaken the field of the armature transverse reaction by decreasing magnetic conductivity of the magnetic circuit in the transverse direction. Therefore, such a structure lacks commutating poles and a compensation winding. There are no permanent magnets in the structure, all windings are stationary, an electronic switch is used instead of a collector, and a windingless low-inertia rotor does not require additional measures to remove heat. That all has made it possible to significantly reduce the cost of active materials for the traction engine and improve its reliability.

To test the performance of the new design, a full-size model of the engine and a working experimental prototype were fabricated. Applying a synchronous jet engine with magnetization for the BMW i3 electric car as an analog, the engine calculations were performed and its simulation was carried out. The results of the analysis show that the mass of the new engine is 35 % greater than the mass of the analog but the cost of active materials is less than that of the analog by 63 %. The results testify to the possibility of implementing a given structure industrially

Keywords: DC motor, armature transverse reaction, number of pole pairs, switch

DESIGN OF A DIRECT CURRENT MOTOR WITH A WINDINGLESS ROTOR FOR ELECTRIC VEHICLES

Dmytro Ivliev
Corresponding author
PhD, Associate Professor*
E-mail: ivlevd@opu.ua

Volodymyr Kosenkov
PhD, Professor, Head of Department
Department of Physics and Electrical Engineering
Khmelnytskyi National University
Instytut's'ka str., 11, Khmelnytskyi, Ukraine, 29016

Oleksandr Vynakov
PhD, Associate Professor*

Elvira Savolova
Senior Lecturer*

Viktoria Yarmolovych
Senior Lecturer*

*Department of Electromechanical Engineering
Odessa Polytechnic State University
Shevchenka ave., 1, Odessa, Ukraine, 65044

Received date 19.05.2021 **How to Cite:** Ivliev, D., Kosenkov, V., Vynakov, O., Savolova, E., Yarmolovich, V. (2021). Design of a direct current motor with a windingless rotor for electric vehicles. *Eastern-European Journal of Enterprise Technologies*, 4 (5 (112)), 41–50.
Accepted date 17.07.2021 doi: <https://doi.org/10.15587/1729-4061.2021.231733>
Published date 31.08.2021

1. Introduction

In more than a century of their history, electric cars have experienced two ups and one downturn. The serial passenger electric vehicles were first produced in 1907; for several decades, they became leaders of the automotive industry. However, by 1935, electric cars were completely displaced from the market by vehicles with an internal combustion engine. In 50 years, interest in electric cars has revived again, and the beginning of the 21st century witnessed a new rise.

Throughout the 20th century, the main traction engine for electric vehicles was a direct current motor (DCM) but, as power electronics developed, it began to lose its position. Fig. 1 shows the percentage of the use of three types of electric motors in 44 models of electric vehicles whose global sales began in the period from 2005 to 2012 [1].

The diagram demonstrates that by 2008 DC motors were completely displaced from the automotive drive market.

Due to its advantages such as ensuring a constant torque over a wide range of speeds, high overload ca-

capacity, wide possibilities for adjusting excitation (parallel, serial, mixed), DCM most fully corresponds to the tasks of the traction electric drive. Its characteristics are still largely the benchmark for any solutions in this area.

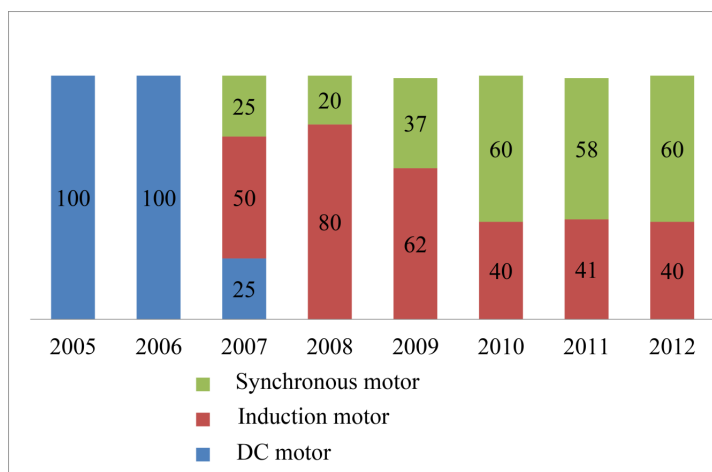


Fig. 1. The dynamics of application of different types of electric motors

However, its shortcomings, namely the presence of an unreliable collector unit, high cost, and large mass do not allow it to take its rightful place among modern high-tech electric vehicles. Therefore, it is a very relevant task to design new DCM structures in which the shortcomings of classical DC machines are minimized.

2. Literature review and problem statement

The review reported in [1] shows that 60 % of all traction motors installed in electric vehicles are synchronous (Fig. 1). According to the type of excitation, synchronous motors can be divided into three main groups:

- motors with electromagnetic excitation;
- motors with surface-placed permanent magnets;
- motors with incorporated permanent magnets.

According to [2], the most popular in the market of traction drives of electric vehicles are synchronous motors with incorporated permanent magnets. This conclusion is confirmed by the review of traction engines from the world’s largest manufacturers of electric vehicles (Nissan, Tesla, Honda, Toyota, Chevrolet, BMW), given in [3].

However, in 2020, a new trend emerged in the traction drive market: the transition from magnetoelectric excitation to electromagnetic excitation.

Thus, the BMW i3 model of 2016 is equipped with a hybrid synchronous motor with permanent magnets [4]. However, for the next model of the iX3 2020, BMW designers installed a traction synchronous motor with electromagnetic excitation [5]. Bentley is also developing in the same direction; in August 2020, it announced its participation in the OCTOPUS program to build a new electric car power unit without the use of permanent magnets [6]. One can also add Renault here; it initially equips all its electric cars of the Berlingo and Zoe brands only with synchronous engines with electromagnetic excitation.

The main reason for such activities is the ever-increasing cost of high-cost neodymium magnets. According to experts, it currently accounts for 30÷60 % of the total cost of active materials for the electric motor [7, 8]. According to forecasts [9], given a growing demand, there may be a shortage of permanent magnets in 2030 and a significant increase in their cost. The issue of abandoning the use of the expensive rare earth metals neodymium and dysprosium for permanent magnets is given great attention by the state structures in the largest industrialized countries. The U. S. Department of Energy’s Advanced Research Agency launched the REACT (Rare Earth Alternatives in Critical Technologies) program in 2011 [10]. The program was attended by 14 universities and national laboratories in the United States, as well as 27 universities and corporations as partners of the program. Work on the creation of permanent magnets without rare earth elements is carried out not only in the United States but also in the European Union where there is a program “EURARE” (European Rare Earth Project) [11]. Work in the same direction is underway in Japan where

the state program “Development of Magnetic Materials for High-Efficiency Motors” was launched in 2014 [12].

One way to resolve the issue of the increasing cost of permanent magnets is to abandon their use and return to electromagnetic excitation in electric vehicle traction motors. However, this requires that electromagnetically excited motors should provide for efficiency comparable to that of magnetoelectric excitation motors.

It is known that the traction characteristic of the automobile drive has two characteristic regions: a constant torque in the range $n=0\div n_{rat}$ and constant power in the range $n=n_{rat}\div n_{max}$.

Typically, in modern traction engines, $n_{rat}=5,000$ rpm, $n_{max}=12,000$ rpm. A high rated speed of the traction engine is necessary to reduce its dimensions and improve efficiency. However, it is impossible to maintain high efficiency over the entire speed range, which is why, when analyzing the modes of operation of the engine in various driving cycles such as urban, suburban, highway, designers opt for a compromise option. At the initial design stage, with a fixed value of the outer diameter, an engine is optimized by selecting the number of pole pairs. In modern traction engines, this parameter is within $p=4\div 6$ [13].

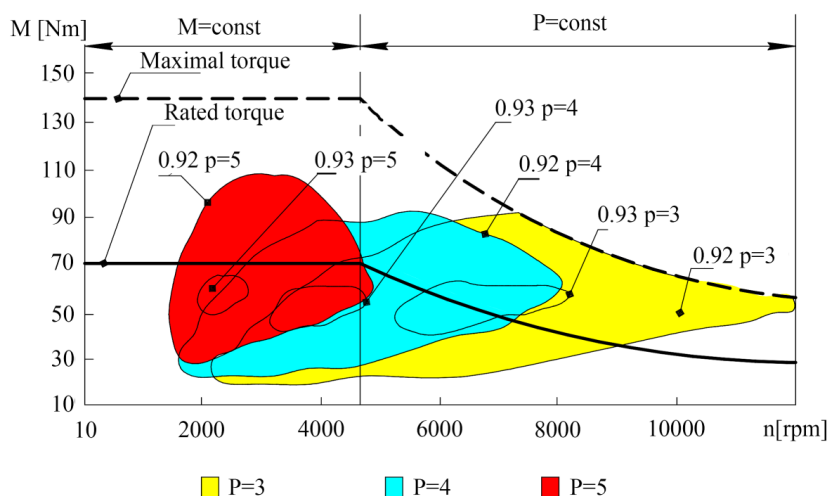


Fig. 2. Traction characteristics

Paper [14] reports data on the influence of the number of pole pairs on the efficiency of the traction motor (Fig. 2).

Analysis of the efficiency fields constructed according to [14] reveals that modern traction motors are optimized to work with maximum efficiency either in the zone of constant torque $p=5\div 6$, or in the middle zone $p=4$. According to [13], the rotor outer diameter in engines for the Toyota Prius (Japan), Nissan Leaf (Japan), and BMW i3 (Germany) models is within $D_{or}=130\div 180$ mm.

Due to the large size of the excitation windings, it is impossible to arrange 12 pronounced poles within such a small volume, a maximum of 4 or 6 (Fig. 3, 4) [15, 16]. However, if one uses permanent magnets, 5 mm high, instead of a copper winding, this would not cause any difficulties (Fig. 5) [17].

Based on these considerations, we can conclude that automotive engines with electromagnetic excitation are well optimized for operation at high speeds but inferior in efficiency to motors with magnetoelectric excitation at low speeds.



Fig. 3. The rotor of Renault Zoe, $p=2$



Fig. 4. The rotor of BMW iX3, $p=3$



Fig. 5. The rotor of BMW i3, $D_{or}=180$ mm, $p=6$

For motors with electromagnetic excitation, this disadvantage can be eliminated. The issue related to small pole division has been known for a long time; it was solved in the middle of the 19th century with the advent of the structure of a synchronous inductor machine (IM).

As one knows, the rotor of the homopolar IM is made in the form of a gear wheel, in which the teeth play the role of windingless poles. The simplest homopolar IM has only one excitation winding, located together with the armature winding in a fixed stator. In this case, the engine with electromagnetic excitation may have the same number of poles as that of a motor with magnetolectric excitation.

In addition, the engine with electromagnetic excitation is devoid of the main drawback inherent in all engines with magnetolectric excitation – the impossibility of adjusting the magnetic flux and the impossibility of disabling it under the emergency modes of engine operation.

In modern traction motors with magnetolectric excitation, this disadvantage is almost eliminated. However, this issue was solved by complicating the structure of the engine and inverter, which, in turn, leads to an increase in the cost of the entire electric drive.

3. The aim and objectives of the study

The aim of this study is to design a DC traction motor with an inductor-type magnetic system for driving an elec-

tric car, which would improve the efficiency and economic attractiveness of this type of electric machines.

To accomplish the aim, the following tasks have been set:

- to fabricate a prototype of the DC motor with a windingless rotor (DCMWR) and test it;
- to design a traction DCMWR for the drive of an electric vehicle, to simulate the distribution of magnetic induction in the working air gap, to analyze the stationary thermal field, to perform weight-size and cost analyses.

4. The study materials and methods

Work on the design and research of DC motors with a windingless rotor with a magnetic system of inductor type [18] has been carried out at the Odesa National Polytechnic University (Ukraine) since 2006.

In DCMWR, similarly to the inductor machine, the value of magnetic induction in the working gap varies only in magnitude, remaining unchanged by the sign. The conversion of energy in DCMWR occurs due to a change in the mutual inductance between the fixed armature windings and excitation when moving the poles of the rotor relative to the stator teeth (Fig. 6).

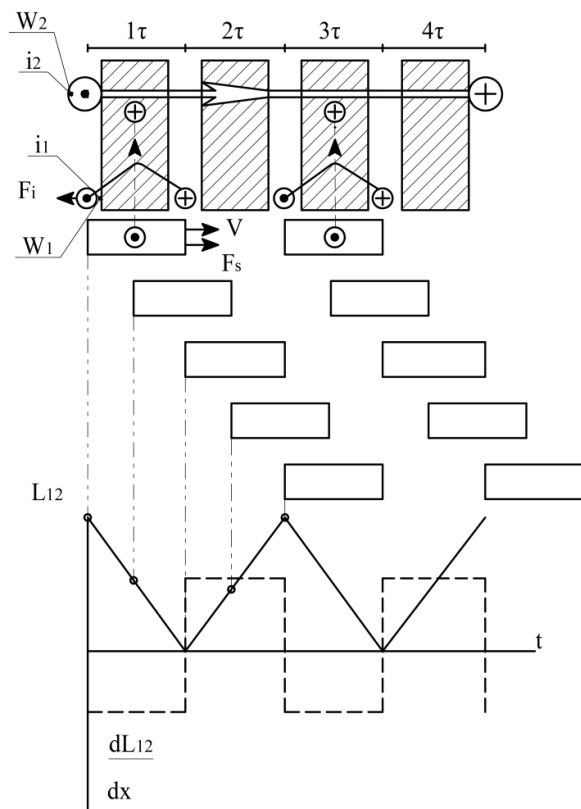


Fig. 6. Flux linkage change

Similar to the inductor machine, only half of the active stator surface is involved in the conversion of energy in DCMWR (Fig. 7), which leads to the need to increase the active length of the section.

However, the copper consumption increases slightly since it is possible to increase the number of pairs of poles in DCMWR from $p=3$ to $p=6$, as a result of which the length of the frontal parts (and, accordingly, the total mass of the winding) decreases.

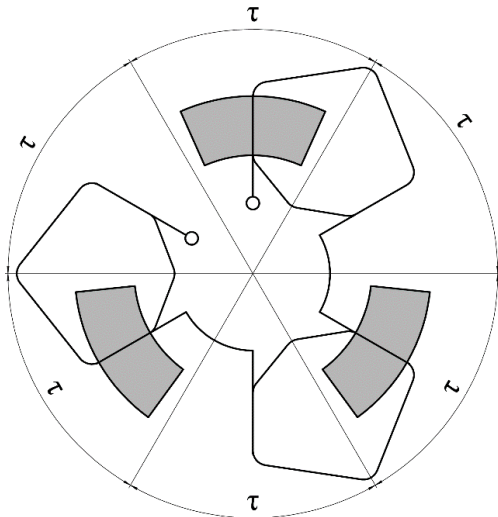


Fig. 7. Prototype sections

To test the operability of the structure, a full-size prototype of DCMWR, end version, was fabricated (Fig. 8, 9). Its rated data are $P_{rat} = 5 \text{ kW}$, $U_{rat} = 220 \text{ V}$, $n_{rat} = 1,500 \text{ rpm}$ ($\omega_{rat} = 157 \text{ s}^{-1}$), $I_{rat} = 25.78 \text{ A}$, $M_{rat} = 72 \text{ Nm}$, $p = 3$, $Z\tau = 6$, $J = 0.0405 \text{ kg}\cdot\text{m}^2$, $m = 80 \text{ kg}$, the magnetic system was made of structural steel, grade St3, instead of electrical steel.

The DCMWR prototype (Fig. 9–11) is a two-stator end electric machine of the axial type whose distinctive feature is the absence of a common yoke.



Fig. 8. General view of the prototype

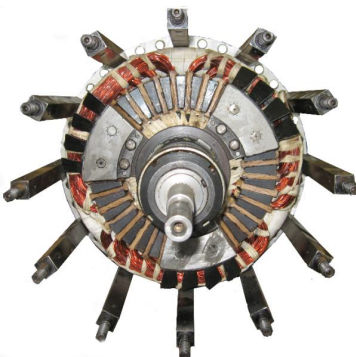


Fig. 9. Inside view of the prototype

The DCMWR magnetic system consists of a series of magnetically uncoupled steel segments of the U-shaped type 1, fixed in non-magnetic (aluminum) end shields 5,

between which there are the windings of rotor 2. In the grooves between the segments of each stator are the sections of armature winding 3. All segments of each stator are covered by a common exciting winding 4.

In such a structure, all stator grooves are open on both sides (Fig. 8, 10), which makes it possible to significantly weaken the field of the armature transverse reaction Φ_a by reducing the magnetic conductivity of the magnetic circuit in the transverse direction. Therefore, in a given structure there is no need to install commutating poles and a compensation winding.

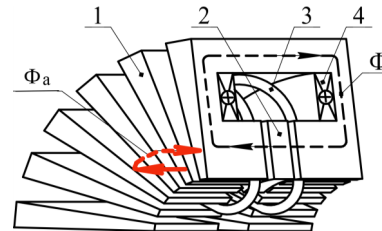


Fig. 10. Prototype axonometry

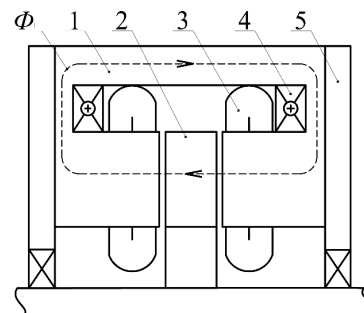


Fig. 11. Prototype cross-section

The structural scheme with a segmented stator and a one-piece rotor (Fig. 10) is used in DCMWR with a maximum rotational speed of 1,000–1,500 rpm. To limit the response of the armature in high-speed machines, a structural scheme with a one-piece stator and a segmented rotor is preferable (Fig. 12). Common to the two structural schemes are the ways of limiting the armature reaction, shown below by using the structure with a common stator as an example.

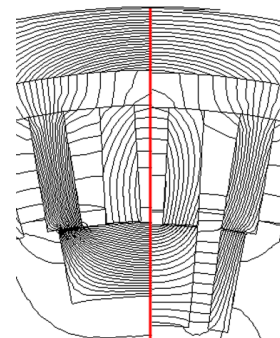


Fig. 12. Stator with wide grooves and a small working air gap

The first technique involves the presence of a stator with wide open grooves. In this case, the magnetic resistance of the air gap increases due to the lack of closure along the crowns of the teeth, its value can be chosen as minimal-

ly technologically possible (Fig. 12, left side).

The segmented pole, whose area is equal to the area of the non-segmented pole, further weakens the reaction field of the armature (Fig. 12, right side).

An attempt to use this approach in a stator with narrow semi-closed grooves and a small air gap, where the closure of the armature field proceeds along the crowns of the teeth, is guaranteed to lead to the overturning of the field (Fig. 13, left side).

Therefore, with a small width of the groove, it is necessary to increase the value of the working air gap (Fig. 13, right side). This approach is generally accepted for DC machines; thus, an industrially produced DCM with a power of $P=200$ kW has an air gap of $\delta=3$ mm.

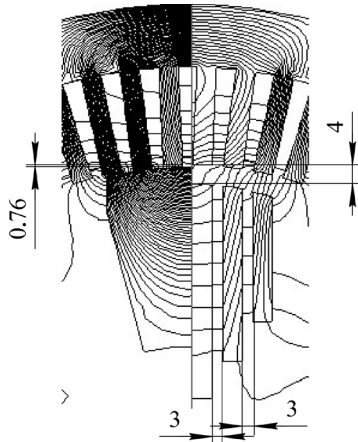


Fig. 13. Stator with narrow grooves and a large working air gap

5. The results of studying a DC motor with a windingless rotor

5. 1. The prototype of a DC motor with a winding rotor of end design

Since the magnetic system of the prototype is made of structural steel, grade St3, the DCMWR tests were carried out in a limited manner. The tests included checking the operability of the structure and the technique for limiting the reaction of the armature; the acquisition of the waveform of start and reverse, the acquisition of the traction characteristic; thermal tests, checking the operation with the reversed collector and an electronic switch.

Based on the results of the tests, the following conclusions were drawn.

The DCMWR structure is fully operational. The segmented stator makes it possible to significantly weaken the field of the transverse reaction of the armature, thereby increasing the overload capacity of the engine for current (Fig. 14).

The nature of the DCMWR dynamic processes fully corresponds to the similar characteristics of the classical DC machine (Fig. 15).

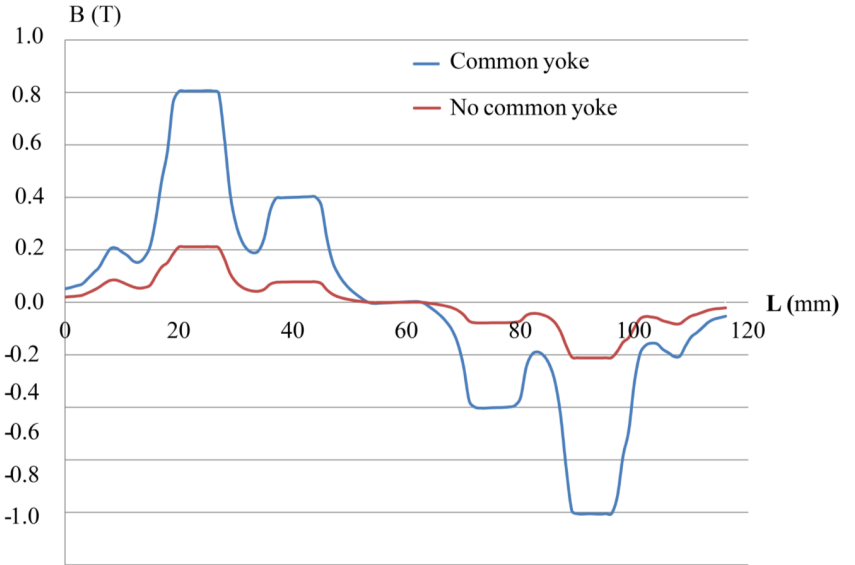


Fig. 14. Distribution of the magnetic induction of the armature field in the working air gap over τ

At the same time, one should note the complete coincidence between the values of the electromechanical constant T_M , determined from the following equation:

$$T_M = j \cdot \frac{\omega_0}{M_{rat}} = 0.0405 \cdot \frac{176}{72} = 0.1 \text{ s}, \quad (1)$$

and the value of T_M derived from the waveform, where the start-up time is $t_s=0.32$ s, and

$$T_M \approx \frac{t_s}{3} = \frac{0.28}{3} = 0.09 \text{ s}. \quad (2)$$

The traction characteristic $M=f(I)$ (Fig. 16) was acquired with the rotor braked, which was fixed in the predefined position, then, as the armature current changed at the rated excitation current, the counting involved the dynamometer scale.

The analysis of the characteristic demonstrates that the experimental curve is lower than the estimated one, which relates to the rapid saturation of the elements of the magnetic circuit of the engine made of structural steel, St3. However, even in this version, the possibility of a 2+2.5-multiple current overload is provided. With a much smaller mass of rotating parts than that in a typical analog, this ensures the increased performance and energy savings under dynamic modes.

Based on the results of DCMWR thermal tests and modeling its stationary thermal field, the excess temperature of the exciting winding $T_{ew}=50$ °C and the armature winding $T_{aw}=62$ °C above the ambient temperature $T_a=21$ °C were determined. The comparative analysis [19] reveals that DCMWR with natural cooling removes heat more efficiently than an analog with self-ventilation.

Initially, the DCMWR prototype tests were carried out with a reversed collector, in which the brush assembly, fixed on the shaft, rotated relative to the fixed collector fixed on the end panel. The obvious advantage of this approach is the ability to work from an alternating current network with a cheap control circuit based on a thyristor rectifier. Subsequently, the collector was replaced with an electronic switch. Fig. 17 shows a diagram of the twelve-section winding of the DCMWR prototype, where IGBT transistors are used as power keys.

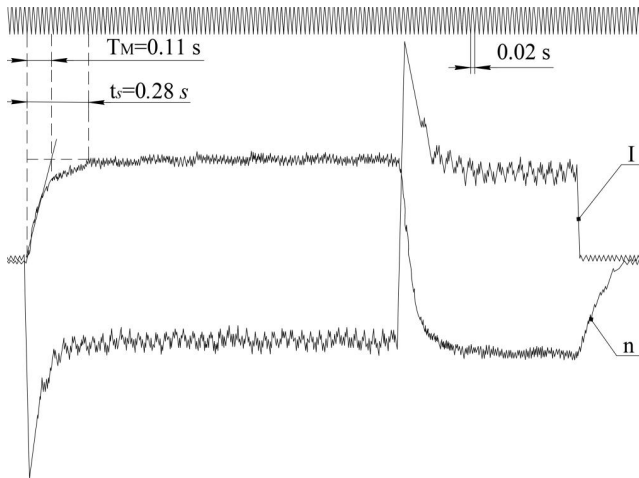


Fig. 15. Oscillograms of the prototype start and reverse

The scheme works as follows. Let the position of the poles be such that the rotor position sensor (RPS) opens the VT1 and VT14 keys. Then the current would pass along the following path: the plus terminal of a power supply, the VT1 key, sections C1-C6 (the first parallel branch), as well as parallel C12-C7 (the second parallel

branch), the VT14 key, the minus terminal of a power supply. In this case, the rotor would turn and RPS would close the keys VT1, VT14, and turn on the keys VT3, VT16 (or VT23, VT12 when moving the rotor in the other direction). When one turns on the keys VT3, VT16, the direction of current in sections C1 and C7 would change to the opposite. With further rotation of the rotor, the signals from RPS would enable the next pairs of transistor keys and, when moving the engine at 2τ , a full cycle of switching electronic keys would occur.

After analyzing the results obtained, the next stage began, namely, the design and manufacture of a full-fledged experimental sample of a low-speed DC generator with a one-piece windingless rotor and a segmented stator. A given generator, $P_{rat}=1$ kW, $U_{rat}=300$ V, $n_{rat}=600$ rpm, is designed to work as part of a wind power plant: the diameter of the internal boring of the stator $D_a=140$ mm, the number of pole pairs $p=6$ (Fig. 18-20) [20].

To design the generator, we devised a procedure for calculating low-speed electric machines of this type and determined the optimal values of electromagnetic loads and geometric ratios.

The full cycle of tests has confirmed the correctness of the calculation procedure and the match between the estimated and experimental data.

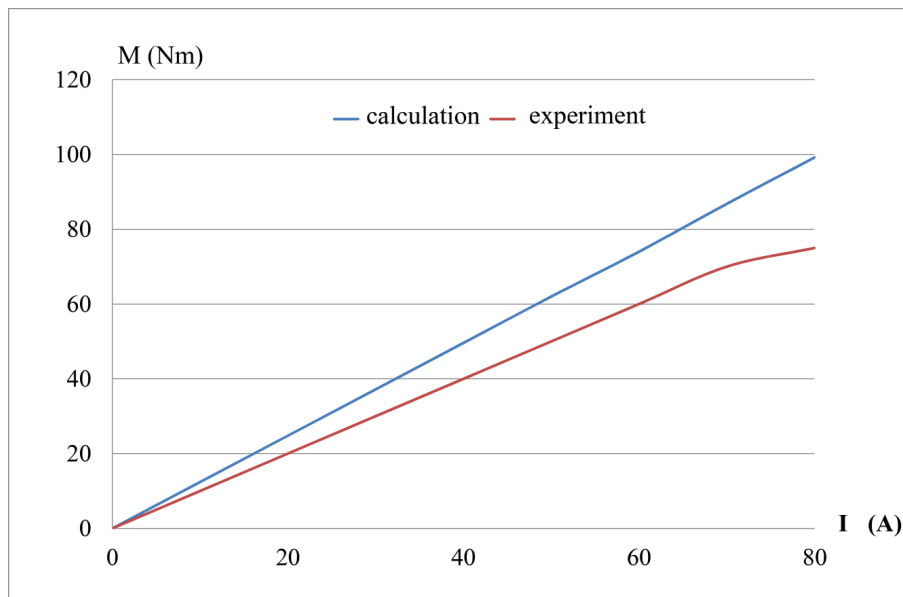


Fig. 16. The prototype torque (traction) characteristic

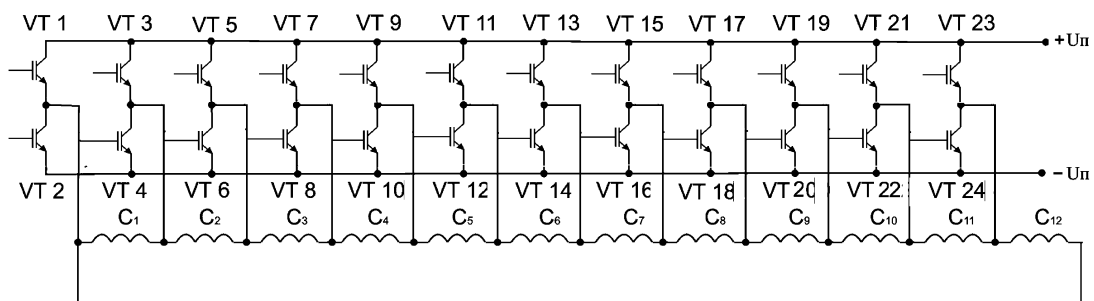


Fig. 17. The prototype switch diagram

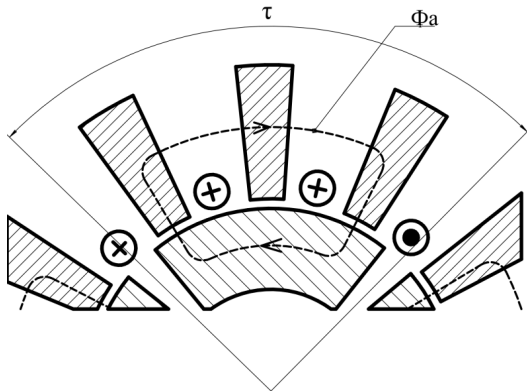


Fig. 18. Segmented stator



Fig. 19. Generator general view



Fig. 20. Rotor $D_a=140$ mm, $p=6$

5. 2. A high-speed DC motor with a windingless rotor

The experience gained in designing a prototype, as well as taking into consideration the identified shortcomings, have allowed us to proceed to the next stage of DCMWR research – the development of a high-speed engine to work as part of an electric car drive.

As one knows, the maximum speed of rotation of an electric machine is limited by two factors: the mechanical strength of the rotor and the increasing losses in steel. The stator of a high-speed electric machine must withstand significant tangential forces and have a relatively small mass to reduce losses in steel.

The structure of the segmented stator of the low-speed DCMWR (Fig. 18) does not meet these requirements. For high-speed machines, a structural scheme with a one-piece stator and a segmented rotor is preferable (Fig. 21, 22). In both cases, the weakening of the field of the transverse reaction of the armature is achieved. However, in the second case, the consumption of electrical steel is less.

The DCMWR body 1 is part of the magnetic system and is made of massive conventional structural steel. Massive

are the rotor poles 5. Only the stator 4 package is made of electrical steel, in which the armature winding 3 is laid. The stator package has a relatively small mass (due to the low height of the yoke) and is assembled from sheets of electrical steel of the powercore 020-130Y320 grade with a thickness of 0.02 mm. Exciting winding 2 is located inside the body and is stationary. Such a structural solution is classic for the homopolar inductor machines.

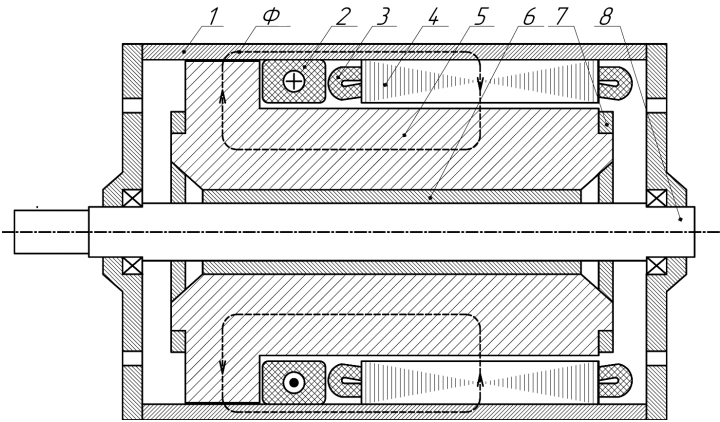


Fig. 21. High-speed engine: side view

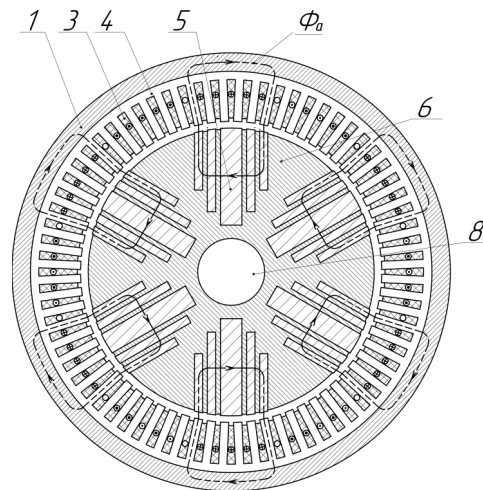


Fig. 22. High-speed engine: front view

The DCMWR segmented rotor is structurally similar to the collector-type prefabricated rotor with prismatic permanent magnets (CRPPM) [21]. CRPPM is used in the high-speed electric machines for aircraft with speeds of $30 \cdot 10^3 \div 60 \cdot 10^3$ rpm. The DCMWR rotor consists of a non-magnetic body 6, fixed on shaft 8, in the grooves of which the segments of poles 5 are laid. To counter centrifugal forces, the DCMWR rotor, like the CRPPM rotor, has a bandage shell made of composite material, shaped in the form of a solid non-magnetic sleeve, 2 mm thick, and an additional composite end bandage 7.

As an analog for DCMWR, a synchronous jet engine with magnetization installed in the 2016 BMW i3 electric car was chosen. The choice of a given analog is due to the fact that its characteristics are well known [3, 4], in particular from open reports by Tim Burress from the Oak Ridge National Laboratory, USA [17, 22].

Based on the data given in those sources, the following parameters were adopted for the DCMWR calculation: the inner diameter of the stator $D_{si}=180$ mm, the number of pole pairs $p=6$, the number of stator grooves $Z=72$; an indirect liquid cooling.

The values for the linear current density $A=11 \cdot 10^4$ A/m and current density $j=12$ A/mm² with indirect liquid cooling are adopted on the basis of the recommendations given in [23] where modern methods of cooling electric machines are considered.

As one knows, losses in steel increase dramatically with increasing frequency. Based on the recommendations for the design of inductor machines, the following flux density values were adopted – for the air gap $B_\delta=0.4$ T, for the teeth $B_t=0.8$ T.

Since the analog has a large number of toothed divisions into poles and narrow grooves, the transverse reaction of the armature is restricted according to the second technique (Fig. 13, right side), which implies the presence of a large working air gap.

In DCMWR, $B_\delta=0.4$ T, which makes it possible with relatively low costs for weight and losses to increase the working air gap to $\delta=4$ mm (Fig. 13, right side). In addition, the large air gap makes it easy to place a rotor bandage made of carbon fiber.

Based on the accepted initial data, a high-speed DC motor with a windingless rotor was calculated. The comparison of the DCMWR and analog is given in Table 1.

Table 1

Comparative data on the DCMWR and analog

Parameter	Unit	BMW i3	DCMWR	%
Maximal values				
Power P_{max}	kW	125	121.5	–
Torque M_{max}	Nm	250	258	–
Maximal speed n_{max}	rpm	11.400	11.400	–
Rated values				
Rated power P_{rat}	kW	75	75.3	–
Rated torque M_{rat}	Nm	–	159.9	–
Rated speed n_{rat}	rpm	4.500	4.500	–
Voltage range	V	250–400	250–400	–
Rated efficiency	%	97	94	–3 %
Linear current density A	A/m	–	$11 \cdot 10^4$	–
Air gap flux density B_δ	T	–	0.4	–
Teeth flux density B_t	T	–	0.8	–
Current density in armature winding j	A/mm ²	–	12	–
Stator outer diameter D_{so}	mm	242	250	+3 %
Stator inner diameter D_{si}	mm	180	180	–
Stator length	mm	132	167	+21 %
Assembled engine weight	kg	42	64	+35 %

The estimated data for our weight and size analysis are given in Table 2. Prices for materials are in 2015; taken from [24]; the price of structural steel is accepted as half the price of electrical steel.

In addition to the calculation, the DCMWR stationary thermal field was simulated (Fig. 23), as well as the distribution of magnetic induction in the DCMWR working air gap (Fig. 24).

Table 2

Weight and cost of active materials

Parameter	Unit	BMW i3	DCMWR	%
Mass				
Electrical steel mass	kg	21.9	13.2	–40 %
stator m_s	kg	13.7	13.2	–4 %
rotor m_r	kg	8.2	–	–
Structural steel mass	kg	–	28.6	–
DCMWR body m_b	kg	–	8.3	–
DCMWR rotor poles m_p	kg	–	20.3	–
Winding copper mass	kg	7	13	+46 %
armature winding m_{aw}	kg	7	9	+22 %
DCMWR exciting winding m_{ew}	kg	–	4	–
Permanent magnet mass	kg	2	–	–
Price (*)				
Electrical steel	EUR	19.71	11.88	–40 %
Structural steel	EUR	–	12.87	–
Winding copper	EUR	49	91	+46 %
Permanent magnets	EUR	240	–	–
Total	EUR	308.71	115.75	–63 %

Note: (*) Electrical steel=0.90 EUR/kg; structural steel=0.45 EUR/kg; winding copper=7 EUR/kg; permanent magnets NdFeB=120 EUR/kg

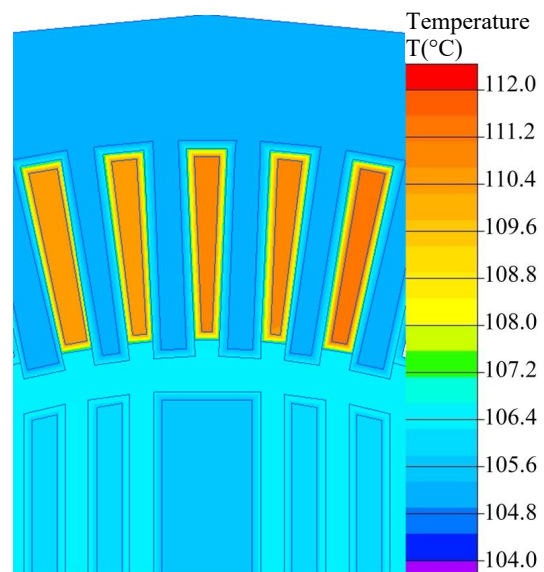


Fig. 23. Temperature distribution in a high-speed engine

Our results allow for a preliminary assessment and identification of the strengths and weaknesses of the new design.

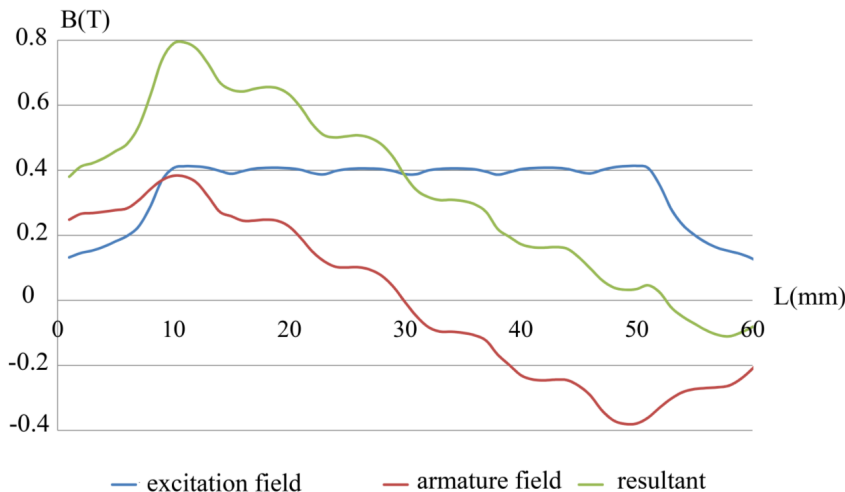


Fig. 24. Distribution of magnetic induction in the working air gap of a high-speed engine

6. Discussion of results of designing a DC motor with a windingless rotor for use in electric vehicles

Unlike its counterpart, in DCMWR only 50 % of the usable area of the stator is involved in energy conversion. Provided that the dimensions of the internal diameters of the DCMWR and analog stators were equal, it could be expected that the length of the DCMWR stator package would increase by 50 %; in reality, the increase was only 21 % (Table 1). This difference is because open sources lack accurate information on the values of electromagnetic loads, induction values, and the coefficient of pole overlap of the analog. The increase in the values of these parameters led to a decrease in the length of the stator.

Our analysis of the DCMWR stationary thermal field has revealed that at the accepted values of electromagnetic loads under the rated mode of operation, the absolute values of the temperatures of the structural elements do not exceed the permissible values for the insulation class H (Fig. 23).

A comparative analysis of the DCMWR and analog (Table 1) once again confirms that the engine with magneto-electric excitation is better than the engine with electromagnetic excitation in terms of weight and energy indicators. While the value of DCMWR efficiency is inferior to the analog by only 3 %, in terms of weight it is heavier than the analog by 35 % (Table 1).

At the same time, the comparison of the cost of active materials for the DCMWR and analog (Table 2) shows that the analog is more expensive than DCMWR by 63 %. Based on the analysis of the cost of permanent magnets given above, we can conclude that soon the price gap between

engines with electromagnetic and magneto-electric excitation will only grow.

Our simulation of the distribution of magnetic induction in the working air gap demonstrated that a given structure can withstand a 2-3x current overload due to a significant weakening of the field of the armature transverse reaction. Fig. 24 shows the distribution of magnetic induction in the DCMWR working air gap for the rated mode of operation. The shape of the curves fully corresponds to similar curves of a classical DC machine. As can be seen, with an increase in the working air gap due to the pulsations of the magnetic flux due to the toothing of the stator decrease.

The DCMWR design makes it possible to fully automate the assembly process of a given engine and minimize the time of its manufacture, which is an

important requirement in the manufacture of traction motors for electric vehicles. In the future, such a structure can be produced industrially.

It should be noted that the currently existing optimized design procedure for low-speed DCMWR does not make it possible to optimize the structure of high-speed DCMWR. Optimization of the design of a high-speed DC motor with a windingless rotor is the subject of further research.

7. Conclusions

1. Our tests of the prototype have shown that DCMWR, like any other electric machine, has its advantages and disadvantages. However, in comparison with the disadvantages of a classic DC machine, the disadvantages of DCMWR are not so significant. The absence of a collector, commutating poles, and a compensation winding, low inertia, 3-fold overload capacity, and a rotor from which there is no need to remove heat, neutralize its disadvantage associated with the need to increase the length of the rotor. In comparison with synchronous motors with electromagnetic excitation, DCMWR is more effective than analogs under the modes with a high torque value due to the possibility to increase the number of pairs of windingless poles.

2. The simulation results, as well as the weight and size and cost analyses, demonstrate that in terms of its energy performance, DCMWR is close to an analog. Inferior to the analog by 3 % in efficiency, DCMWR is, at the same time, cheaper than the analog by 63 % in terms of the cost of active materials.

References

1. De Santiago, J., Bernhoff, H., Ekergerd, B., Eriksson, S., Ferhatovic, S., Waters, R., Leijon, M. (2012). Electrical Motor Drivelines in Commercial All-Electric Vehicles: A Review. *IEEE Transactions on Vehicular Technology*, 61 (2), 475–484. doi: <https://doi.org/10.1109/tvt.2011.2177873>
2. Sarlioglu, B., Morris, C. T., Han, D., Li, S. (2015). Benchmarking of electric and hybrid vehicle electric machines, power electronics, and batteries. 2015 Intl Aegean Conference on Electrical Machines & Power Electronics (ACEMP), 2015 Intl Conference on Optimization of Electrical & Electronic Equipment (OPTIM) & 2015 Intl Symposium on Advanced Electromechanical Motion Systems (ELECTROMOTION). doi: <https://doi.org/10.1109/optim.2015.7426993>

3. Staton, D., Goss, J. (2017). Open Source Electric Motor Models for Commercial EV & Hybrid Traction Motors. MDL. Available at: <https://docplayer.net/64747945-Open-source-electric-motor-models-for-commercial-ev-hybrid-traction-motors-dr-david-staton-dr-james-goss.html>
4. Merwerth, J. (2014). The hybrid-synchronous machine of the new BMW i3 & i8. Available at: http://hybridfordonscentrum.se/wp-content/uploads/2014/05/20140404_BMW.pdf
5. Specifications of the BMW iX3, valid from 07/2020 (2020). Available at: <https://www.press.bmwgroup.com/global/article/detail/T0314265EN/specifications-of-the-bmw-ix3-valid-from-07/2020?language=en>
6. Bentley motors looks to the future of electric drive (2020). Bentley Motors. Available at: <https://www.bentleymedia.com/en/newsitem/1128-bentley-motors-looks-to-the-future-of-electric-drive#images>
7. Burrett, T. (2015). Non-Rare Earth Motor Development. ORNL. Available at: https://www.energy.gov/sites/prod/files/2015/06/f24/edt062_burrett_2015_o.pdf
8. Dorrell, D. G., Knight, A. M., Popescu, M., Evans, L., Staton, D. A. (2010). Comparison of different motor design drives for hybrid electric vehicles. 2010 IEEE Energy Conversion Congress and Exposition. doi: <https://doi.org/10.1109/ecce.2010.5618318>
9. Rare Earth Elements: Market Issues and Outlook (2019). Adamas Intelligence. Available at: <https://www.adamasintel.com/rare-earth-market-issues-and-outlook/>
10. Rare Earth Alternatives in Critical Technologies (2011). Advanced Research Projects Agency – Energy. Available at: <https://arpa-e.energy.gov/technologies/programs/react>
11. EuRare Project (2017). NERC. Available at: <http://eurare.org/>
12. Development of Magnetic Materials for High-Efficiency Motors (2014). NEDO. Available at: https://www.nedo.go.jp/english/activities/activities_ZZJP_100078.html
13. Miljavec, D. (2021). D3.2: Report on considered electrical motor technologies, evaluation matrix, concept decision. Available at: http://drivemode-h2020.eu/wp-content/uploads/2021/02/DRIVEMODE_D3.2_Report-on-electrical-motor-technologies_v1.0.pdf
14. Finken, T., Hameyer, K. (2009). Design and optimization of an IPMSM with fixed outer dimensions for application in HEVs. 2009 IEEE International Electric Machines and Drives Conference. doi: <https://doi.org/10.1109/iemdc.2009.5075438>
15. Le nouveau moteur électrique renforce l'excellence mécanique de Cléon. (2015). Auto-innovations. Available at: <https://www.auto-innovations.com/communiquer/417.html>
16. The first-ever BMW iX3 (2020). Available at: <https://www.press.bmwgroup.com/latin-america-caribbean/article/detail/T0311128EN/the-first-ever-bmw-ix3?language=en>
17. FY 2016 Annual Progress Report for Electric Drive Technologies Program (2017). Energy. Available at: https://www.energy.gov/sites/prod/files/2017/08/f36/FY16%20EDT%20Annual%20Report_FINAL.pdf
18. Bulgar, V. V., Yakovlev, A. V., Ivlev, D. A., Ivlev, A. D. (2013). Nizkoskorostnye elektricheskie mashiny postoyannogo toka induktornogo tipa. Odessa: «Bahva», 307.
19. Kosenkov, V. D., Ivliev, D. A., Yakovlev, O. V., Zheliba, T. A. (2015). The analysis of stationary thermal field in the direct-current motor inductor type. Visnyk Khmelnytskoho Natsionalnoho Universytetu, 5 (229), 93–97.
20. Ivliev, D. (2019). Nyzkoshvydkisnyi henerator postiynoho strumu z bezobmotkovym rotorom dlia vitroenerhetychnoi ustanovky. Odessa, 21.
21. Ismagilov, E., Hayrullin, I., Vavilov, V. (2017). Vysokooborotnye elektricheskie mashiny s vysokokoertsitivnymi postoyannymi magnitami. Moscow: Innovatsionnoe mashinostroenie, 248.
22. Burrett, T. (2017). Electrical Performance, Reliability Analysis, and Characterization. ORNL. Available at: https://www.energy.gov/sites/prod/files/2017/06/f34/edt087_burrett_2017_o.pdf
23. Gai, Y., Kimiabeigi, M., Chuan Chong, Y., Widmer, J. D., Deng, X., Popescu, M. et. al. (2019). Cooling of Automotive Traction Motors: Schemes, Examples, and Computation Methods. IEEE Transactions on Industrial Electronics, 66 (3), 1681–1692. doi: <https://doi.org/10.1109/tie.2018.2835397>
24. Ometto, A., Parasiliti, F., Villani, M. (2015). Permanent Magnet-assisted Synchronous Reluctance Motors for Electric Vehicle applications. 9th International Conference «Energy Efficiency in Motor Driven Systems» EEMODS'15. Available at: https://autodocbox.com/Electric_Vehicle/70901524-University-of-l-aquila-permanent-magnet-assisted-synchronous-reluctance-motors-for-electric-vehicle-applications.html